Villagrossi, E., Pedrocchi, N., Beschi, M., & Molinari Tosatti, L. (2018).
A human mimicking control strategy for robotic deburring of hard materials.
International Journal of Computer Integrated Manufacturing, 31(9), 869–880.
https://doi.org/10.1080/0951192X.2018.1447688

A human mimicking control strategy for robotic deburring of hard materials

Enrico Villagrossi[a] and Nicola Pedrocchi[b] and Manuel Beschi[b] and Lorenzo Molinari Tosatti[b]

[a] Instrumentation and Robotics Department, Danieli Automation, via Stringher 4, 33042 Buttrio (UD), Italy;
[b] Institute of Industrial Technologies and Automation, National Research Council of Italy, Via Corti 12, 20133, Milan, Italy;

ARTICLE HISTORY
Compiled January 8, 2018

ABSTRACT

The paper deals with the use of an industrial robot (IR) for the deburring of hard material items (*i.e.*, cast iron items). The control strategies introduced in the paper aim to mimic the human behaviour during the manual deburring. On the base of a force feedback, provided from a 1-axis load cell, the nominal deburring trajectory is adjusted and deformed making multiple repetition until the nominal deburring path is completed and the burr is removed. The removal of thin layers of material allows the robot to operate at high feedrate avoiding spindle stall and without exciting elastics effects on the mechanical structure of the system. The paper compares the human mimicking control solution and a standard industrial approach demonstrating a reduction of the task cycle time and an improvement of the finishing quality.

KEYWORDS
Deburring with robots and Human-Mimicking control strategies and Hard material deburring and Changepoints detection

1. Introduction

The demand of IRs to be used in machining applications is increased during last years (Pandremenos et al. 2011; Lehmann et al. 2013; Rea Minango and Espindola Ferreira 2017). Despite such industrial interest, the percentage of robots specifically sell for material removal operations tends to remain a niche of the IRs market (Iglesias et al. 2015).

The most of the robotics machining applications are focused on ductile materials where the technological requirements are not narrow, *i.e.*, low forces exchanged between the tool and the workpiece (Xi et al. 2017). The same is for the robotic deburring where the tasks addressed are quite always focused on items made by aluminum alloys with low technological requirements (Berselli et al. 2017).

It is worth noting that the production processes adopted for items made by aluminum alloys guarantee high accuracy and repeatability (*e.g.*, die casting or CNC

Corresponding author: E. Villagrossi, e-mail: enrico.villagrossi@gmail.com

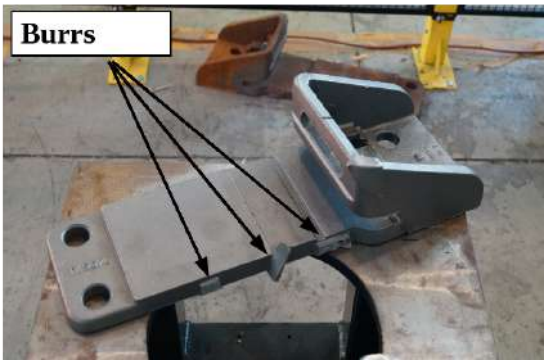

Figure 1. Example of a cast iron item with huge variability in burrs dimensions.

machining). At the same time also the burrs are repeatable in terms of dimensions and position. In such cases, the process quality results in the trajectory optimization, while the tracking error can be neglected. Indeed, the control issues can be easily addressed also adopting mechanical artifacts, such as radially-compliant tool (ATI 2016) to stabilize the contact between the tool and the workpiece.

Conversely, the adoption of IRs in hard material deburring is still challenging and the optimization of the deburring trajectories is not always sufficient. In fact, items made by hard materials, are obtained through less accurate processes (*e.g.*, foundry process) with a consequent lower accuracy. In the same way, also the burrs dimensions and position are hardly predictable (see Figure 1). Thus, the deburring strategies need to be flexible and easily adaptable to the changing of the burrs properties. Nowadays such flexibility requirements are not fully faced from the automatic control strategies and a wide rage of deburring applications are still addressed manually.

The literature on robotic deburring proposes a huge number of control solutions, mainly based on force control strategies, but most of them are still far to be introduced in a real industrial plant. A primary issue is the robustness of the force control algorithms characterized by a large use F/T sensors that require frequent recalibration procedures and do not always guarantee a sufficient reliability. At the same time the purchase cost of the F/T sensors is not negligible if compared to the robot.

A paradigmatic test case is the deburring of cast iron items produced by foundry process (*i.e.*, sand casting). In this case, items are characterized by a huge variability *w.r.t.* the nominal dimensions with burrs of unknown dimensions and placed in an unknown position (Villagrossi et al. 2017). Therefore, the working conditions impose the development of smart control strategies able to merge flexibility and robustness.

2. Literature Review

2.1. *Related works*

The robotic machining and the robotic deburring have to take into account the possible large deformations due to lower stiffness with respect to CNC machines (Abele et al. 2007, 2008; Cen and Melkote 2017). Since late '80s, in order to limit this deflections, many researchers have addressed the robotic deburring dealing with control algorithms. In fact, it is quite common to find deburring algorithms, as in (Kazerooni 1988; Kramer and Shim 1990; Bone et al. 1991; Duelen et al. 1992; Thomessen et al.

1993; Ziliani et al. 2007; X. et al. 2006), based on: impedance control, force control, hybrid force-position control, and contour tracking strategies. Although the feasibility of these techniques is experimentally demonstrated and despite the efforts made by some robot manufacturers (ABB 2016; Fanuc 2016), it is still difficult to find real industrial applications based on such control strategies (Jonsson et al. 2013). A primary problem is related to the complexity that impose the tuning of several control parameters (*e.g.*, the stiffness of the materials). Furthermore, the robustness of the control algorithms can be mined by the necessity of frequent sensor recalibration (*e.g.*, force/torque sensors).

In (Zhang et al. 2006) it was used an hybrid force-visual servoing system able to automatically track a path and generate the trajectory with the robot part-program. In (Song et al. 2012) it was proposed the use of an impedance control strategy to detect the positions of some teaching points. This information are used to: (i) extract the geometrical features of the object, (ii) compare the features extracted with the nominal ones, (iii) calculate the orientation error and (iv) adjust the deburring trajectory. The main drawbacks are related to the cycle time and to the limited number of geometrical shapes that can be reconstructed (*i.e.*, lines and circles). A further evolution of the impedance control can be found in (Song and Song 2013) where two impedance control loops were adopted. The first one acts to maintain stable the contact force along the normal direction *w.r.t.* the deburring surface. The second one acts to provide a compliant motion along the tangential direction in order to remove burrs reliably regardless of their sizes. Therefore, when a high force is applied to the deburring tool because of a large burr, the deburring tool slows down to avoid to exert an excessive force on the workpiece. In this case, the limitation resides in the small dimensions of the burrs that can be machined.

In (Daniali and Vossoughi 2009), it was used a piezoelectric actuator to cope with the burrs variability and to compensate the vibration produced by the technological process. The piezoelectric actuator is controlled through an adaptive critic-based neurofuzzy controller. The limitation is the small range of motion of the piezoelectric actuator that allow to treat burrs with limited dimensions.

Recently, in (Kuss et al. 2016), an Iterative Closest Point (ICP) algorithm was adopted to match the points cloud acquired from a real object and the points clouds derived from all the possible tolerance variations of the nominal model of the workpiece (*i.e.*, the CAD nominal model). The most similar geometrical model was used for the trajectory planning and for the workpiece localization.

2.2. *Industrial practice*

The industries are always looking for robust and effective solutions that are usually far from those described in the scientific literature (see Section 2.1). The industrial solutions for robotic deburring are characterized from weak control algorithms, quite often based on a simple position control. Generally speaking, a possible classification of the control strategies commonly used in industry is:

- simple position control: the robot moves along a predefined trajectory with a constant deburring tool feed rate. The feed rate tool is tuned on a value able to remove the entire burrs (*i.e.*, burrs with fixed dimensions)
  - robustness;
  - lack of flexibility, especially when the burrs dimensions are not fixed;

- feed rate control: the robot moves along a predefined trajectory but the deburring tool feed rate is changed on the base of a force feedback. The force measure can be easily obtained with a 1-axis load cell to measure the force exchanged between the deburring tool and the item, thus, the feed rate of the deburring tool is reduced proportionally
  - higher flexibility *w.r.t.* the use of a constant feed rate (*i.e.*, different size of burrs can be treated);
  - possible productivity decrease. In the case of burrs with big dimensions, the feed rate limit should decrease by becoming unfeasible;

Some issues may arise applying the above mentioned strategies to hard materials. In particular, a single step burr removal (*i.e.*, thick layer of material to be removed) can cause:

(1) the onset of vibrations due to the deburring tool feed rate. There is not only a maximum feed rate limit, but also a minimum feed rate limit to be controlled in order to avoid triggering vibrations;
(2) high forces exchanged between the deburring tool and the burr can cause spindle stall;
(3) high forces exchanged between the deburring tool and the burr can produce a deflection of the mechanical structure of the spindle as depicted in Figure 2. Such deflection can produce a not complete removal of the burr as shown in Figure 3.

3. Contributions

Trying to fill the gap between the robotic research and the industrial practice, the aim of this paper is to present the use of an IR applied in a hard material deburring task where the burrs dimensions and the burrs positions are unknown. At the same time, the robustness and the reliablity of the control algorithm is guaranteed also for high dimensions burrs. The goal is achieved by implementing a human mimicking control strategy able to mimic the worker behaviour during the manual deburring. In case of using abrasive discs, as reported in Figure 5, the worker: (i) optimizes the disc orientation *w.r.t.* the deburring surface, (ii) keeps limited the force exchanged between the deburring tool and the workpiece and (iii) changes the feed rate according with the burr thickness. The force exchanged are kept under control by removing thin layers of material and by repeating the same trajectory several times until the burr is completely removed. In the same way, when the force reach a certain force threshold, the developed algorithm: (i) detaches the deburring tool, (ii) applies a constant offset to the nominal trajectories and (iii) repeats the deburring trajectory until the burr is completely removed. Such approach allows to stabilize the contact force keeping limited the force on the mechanical structure of the spindle avoiding the onset of deflection and elastic effects. In addition, the developed control algorithm changes online the tool feed rate and the orientation of the abrasive disc *w.r.t.* the deburrig surface trying to minimize the robot stiffness. Furthermore, the paper introduces an automatic method for the detection of the force peaks based on the stability analysis of an first order autoregressive (AR1) model. Such solution allows to analyze the force samples contained in a predefined window identifying an AR1 model for each window. The detection of abrupt force variation can be done analyzing the stability of the AR1 model in the considered window. The use of the AR1 model allow to adopt

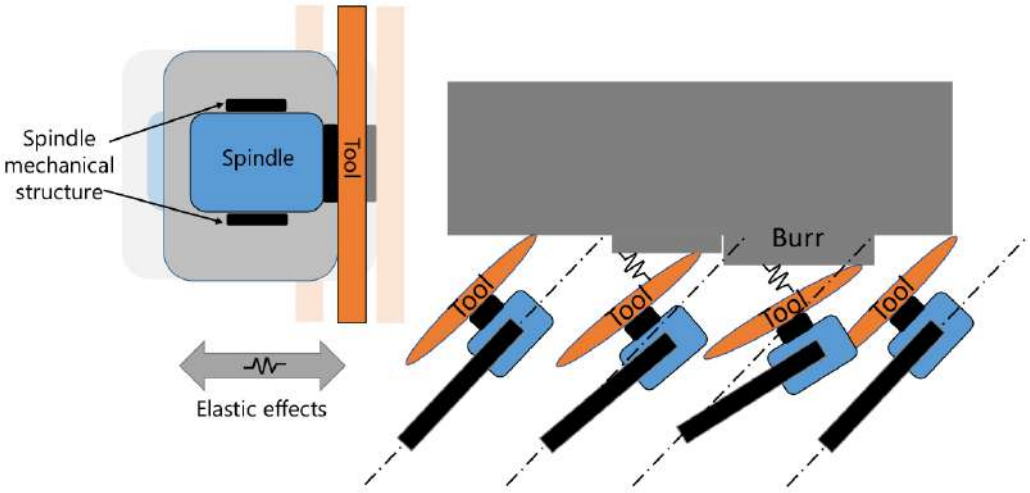

Figure 2. Deflection of the mechanical structure that handle the spindle due to high forces exchanged between deburring tool and workpiece.

Figure 3. Burrs are not completely removed due to the deflection of the mechanical structure of the spindle.

adimensional threshold independent from the material and from the burr dimension.

The paper is organized as follow: Section 3 describes the available setup and the deburring methodology introduced in the paper. The experiment design and the analysis of the results are reported in Section 4. Finally, Section 5 reports the conclusions of the paper.

3.1. *Material*

The available setup, as shown in Figure 4, is based on: a COMAU C5G NJ220-Foundry industrial robot, a manual pneumatic spindle (slightly modified with an *ad-hoc* mechanical structure in order to be handled by the robot) rigidly attached to robot flange, and a 1-axis load cell which is used to measure the deburring force. The deburring tool is an abrasive diamond disc (see Figure 5). The load cell is mounted between the robot flange and the spindle. The control algorithms and the trajectory planner run on an external industrial PC (B&R APC910) while the robot controller manages the low level interpolation of trajectories via-points.

The industrial PC, described in Figure 4 has in charge:

- the control of the deburring tool feed rate sent to the robot controller through a simple TCP/IP channel (control Loop #1, see Figure 6). The control of the feed rate is made online during trajectory execution;

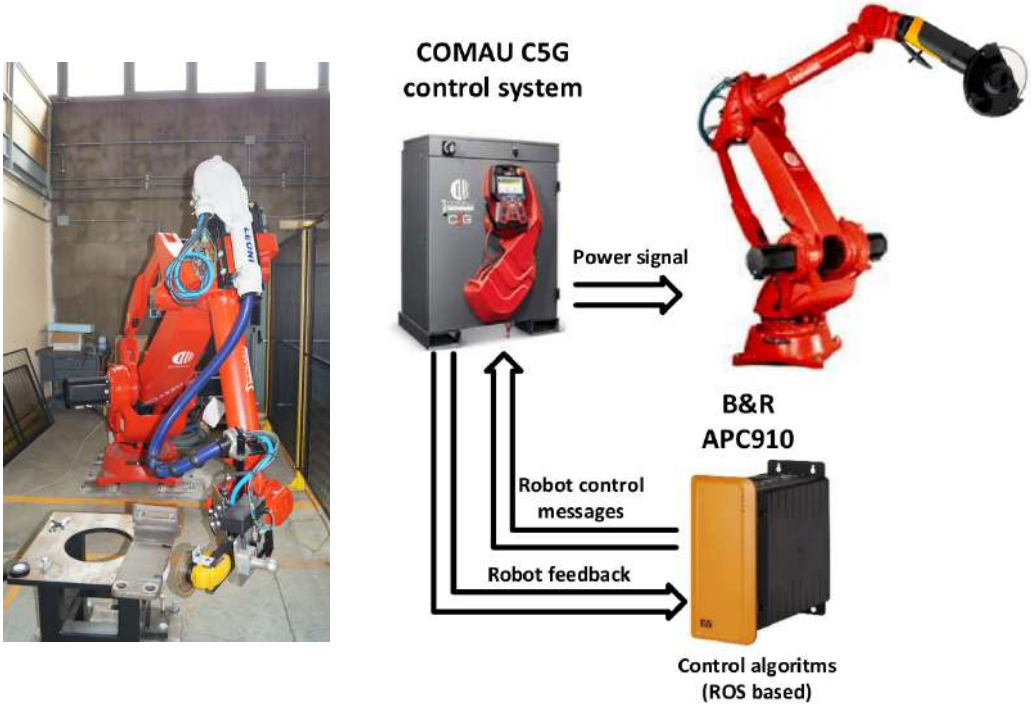

Figure 4. Setup available for the experiments.

Figure 5. Deburring diamond disc.

- the control of the deburring tool orientation sent to the robot controller through the COMAU C5GOpen real-time channel (control Loop #2, see Figure 6). The control of deburring tool orientation is made online during trajectory execution;
- the execution of the deburring trajectories and their relative deformation, *i.e.*, a static offset to be added if the force overcome the threshold F_{th} (control Loop #3, see Figure 6). The trajectory deformation is made offline. The force threshold F_{th} is not directly compared with the force feedback F_f, but it is considered as the average over 50 samples of F_f to avoid the influence of spikes.

Trajectories management is based on the use of ROS[1] Industrial COMAU driver. The communication between the robot and the PC is based on a TCP/IP connection compliant (at the PC side) with ROS-industrial standard[2]. The cycle time of the control node is $1[ms]$. The load cell force feedback, *i.e.*, F_f, is low pass filtered by a 1^{st} order low pass filter and time constant of $0.05[s]$.

3.2. *Deburring with a human mimicking control strategy*

The analysis of the human behaviour during manual deburring can be used to better understand the human control strategies. In fact, a human exerts low forces on the workpiece preferring a multiple repetition of the same movements removing thin layer of material each time (see Figure 9).

As additional control strategy, a human changes continuously the tool feed rate (see Figure 7) and the relative angle between the deburring tool and the workpiece surface adapting the arm stiffness on the base of the thickness of the material to be removed (see Figure 8).

The force exerted by the worker is low, indeed, worker's arms absorb energy acting as passive dampers and stabilizing the process. Conversely, industrial robots provide high inertia, high stiffness, and low damping behavior.

The human approach to deburring can be profitably translated into an IR control strategy with the following advantages:

- reduction of the interaction forces;
- avoidance of the spindle stall;
- reduction of the vibrations of the deburring tool;
- avoidance of deflections of the mechanical structure of the spindle;

3.3. *Methodology*

Trying to mimic the human behaviour, the here proposed deburring control strategy has been designed so that:

- the tool feed rate is adjusted online during the trajectory execution on the base of force feedback;
- the robot kinematics configuration is adjusted online during the trajectory execution to optimize the robotic arm stiffness;
- the contact force is always low also for hard working conditions. If the force

[1]The Robot Operating System (ROS) (OSRF - Open Source Robotic Foundation 2016) is a flexible framework for writing robot software. ROS is nowadays a standard *de-facto* in robotic research.

[2]ROS-industrial (Open Source Project 2016) is the industrial extension of ROS middleware. A ROS-i vendor specific driver, in this case COMAU, enables the control of industrial manipulator through ROS functionalities from an external PC *w.r.t.* the robot control system.

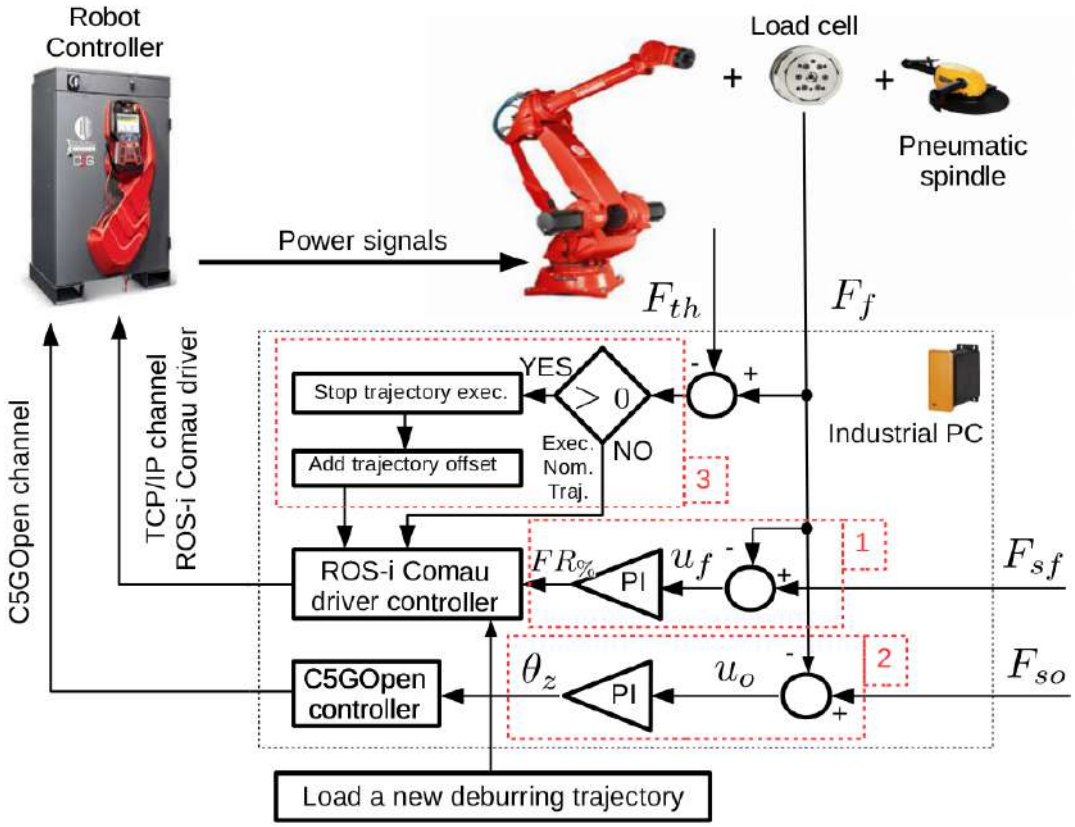

Figure 6. Control scheme that implement the human mimicking deburring strategy.

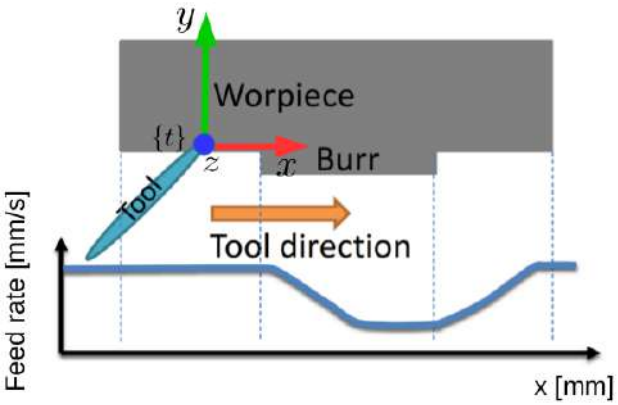

Figure 7. Online control of the deburring tool feed rate on the base of the burr thickness.

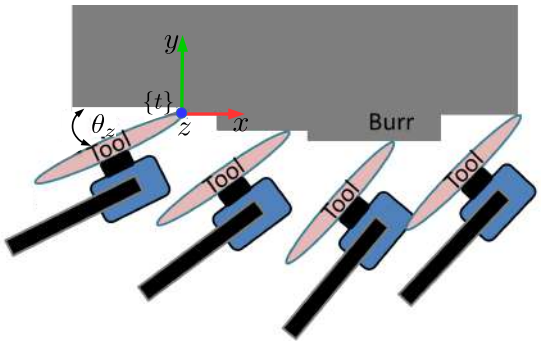

Figure 8. Online adjustment of the robot stiffness through the re-orientation of the deburring tool (angle θ_z) according to the burr thickness.

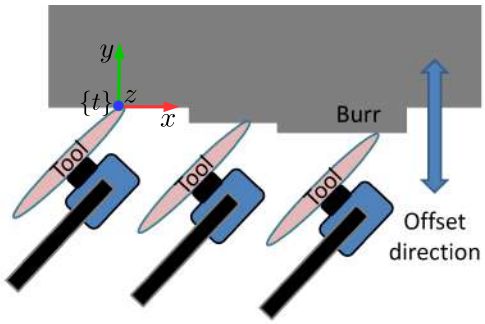

Figure 9. Offset of the deburring trajectory on the base of the force exchanged (offline replanning).

exceeds from a certain threshold F_{th} the robot stops the movement, an offset is added to the nominal trajectory and the new deburring trajectory is executed. The same procedure is repeated until the nominal deburring trajectory can be completed without exceeding the predefined force threshold F_{th}.

Looking at Figure 6 it is possible to denote:

- F_{so}: as the force set-point of the tool orientation control loop;
- F_{sf}: as the force set-point of the tool feed rate control loop;
- F_f: as the force feedback measured by 1-axis load cell;
- $e_o = F_{so} - F_f$: as the force tracking error of the tool orientation control loop;

- $e_f = F_{sf} - F_f$: as the force tracking error of the tool feed rate control loop;

Then, based on the scheme reported in Figure 6, the human mimicking control strategy is implemented exploiting three concurrent control loops:

Feed Rate Control: the Loop #1 controls the feed rate of the deburring tool (see Figure 7) according to the tracking error e_f. The feed rate of the deburring tool is regulated by a simple PI controller and adjusted online during trajectory execution;

Stiffness Control: a deburring application, that exploits a diamond disk, consists on a 4-DoFs task with two additional DoFs (two rotations) that can be freely chosen. The optimization of such free angles can be therefore performed in order to adjust online the robot equivalent stiffness, mimicking the human behavior. In the test case investigated within the paper scope, the elasticity of the robot system is mainly due to the tool support, since the robot used in the experiment is an high-payload robot stiffer than the tool support. In such case, it is easy to see that the equivalent stiffness changes mainly according to the value θ_z (see Fig. 8). For a generic task, however, a proper model of the robot and of the end-effector should be selected according to the properties of the robot, of the tool and of the task. For instance, the use of a milling tool will reduce the residual degrees of freedom just to 1 constraining 5 degrees of freedom of the robot.

The Loop #2 controls the orientation θ_z of the deburring tool according to the tracking error e_o in order to minimize the stiffness when large burrs are detected. Indeed, the minimization of the stiffness allows the system to reduce dramatically the forces and therefore allows to avoid any disk stall. Moreover, the stiffness minimization implies an higher relative damping and therefore Loop #2 is able to stabilize the contact. On the contrary, when the tool is removing small burrs, the stiffness is maximized to increase the system accuracy. The deburring tool orientation θ_z is adjusted during trajectory execution by means of a simple PI controller.

Offset and Repeat: the Loop #3 supervises the maximum force limit. If the force feedback F_f overcomes the force threshold F_{th}, the control loop:

(1) stops the robot movement,
(2) detaches the deburring tool from the workpiece,
(3) adds a static offset to the nominal deburring trajectory and
(4) iterates (adding or removing static offsets) until it is possible to execute the nominal trajectory (see Figure 9).

Despite the simplicity of such procedure, tuning the force threshold F_{th} needs an experimental campaign since it is related to material properties (*i.e.*, the change of the material requires also to re-tune the parameter itself), and to the dimensions of the burrs demanding a long tuning time. To overcome this issue, changepoints detection methodologies (Lavielle 2005; Killick et al. 2012), have been here investigated. Such methodologies were developed in the research field of signal processing to find abrupt changes in a extremely-noised signals considering a short window time of the signal itself.

Among the other available methodologies, the authors have implemented a force Changepoints Detection algorithm based on the Stability analysis of a first-order Autoregressive model (CDSA-AR1). The AR1 model is defined as

$$f_k = \alpha\, f_{(k-1)} + \varepsilon_k \tag{1}$$

where k is time step, α is the autoregressive coefficient, ε_k is a white noise signal.

The model stability is determined by the autoregressive coefficient α. In fact, $|\alpha| \leq 1$ determines stable systems while $|\alpha| > 1$ determines unstable systems.

In order to determine the value of α in a given window, made by the last N elements, it is possible to write the following equation

$$\underbrace{\begin{bmatrix} \tilde{f}_2 \\ \vdots \\ \tilde{f}_N \end{bmatrix}}_{\boldsymbol{F}} = \underbrace{\begin{bmatrix} \tilde{f}_1 \\ \vdots \\ \tilde{f}_{N-1} \end{bmatrix}}_{\boldsymbol{M}} \alpha, \tag{2}$$

where the $f_1, ..., f_N$ are the samples of force recorded in the window. Hence, the autoregressive coefficient α, relative to the window, can be computed by means of a least square regression

$$\hat{\alpha} = \boldsymbol{M}^{+} \boldsymbol{F}. \tag{3}$$

Value of $\hat{\alpha} > 1$ determines unstable systems and therefore the presence of a force changepoint. Such approach allows to analyze an adimensional threshold independent from the material and from the burr dimension.

As final remark, the parameters F_{sf} and F_{so} are easily tunable through a simple automatic procedure that consists of: (i) measure the mean value and the standard deviation of F_f with the free rotation of the tool in order to estimate the bias of due to the disk inertia; (ii) define F_{so} as the measured mean value; (iii) define F_{sf} as the measured mean value plus twice the standard deviation, in order to avoid unwanted speed decrements due to the noise of the force measure.

4. Experiment design

The goal of the experimental session is to compare the results achieved from a standard industrial approach, *i.e.*, constant (slow) feed rate tuned to let the robot able to completely remove the burr, and the result achieved by using the human mimicking control strategy. Two set of experiments were designed:

(1) T1 exploits a simple deburring strategy based on a trajectory executed at constant feed rate. The feed rate is tuned to the maximum feed rate that allows the robot to completely remove the burr without causing spindle stall;
(2) T2 exploits the human mimicking control algorithm (see Section 3.3);

Both the experiments have used:

- the same deburring trajectory;
- workpieces with similar burrs in term of dimensions and number along the path. The dimensions of the burrs removed during the experiments are reported Figure 10.

The tuning of PI controller parameters were optimized given more than 20 deburring experiments, and they result robust *w.r.t.* the burs dimensions, and the item material. The same approach was used for the tuning of the force threshold F_{th}.

The technological parameters used for the experiments are reported in Table 1, while

Figure 10. Burrs dimensions of the workpiece used during the experiment.

	T_1	T_2
$f_v[mm/s]$	1	40
$\Omega[rpm]$	4500	4500

Table 1. Deburrig technological parameters where f_v is the feed rate velocity and Ω is the spindle angular velocity.

$F_{th}[N]$	$F_{sf}[N]$	$F_{so}[N]$
185	178	174

Table 2. Tuning of the control parameters of the human mimicking deburring algorithm. Names are referred to the scheme of Figure 6. F_{th} is the force threshold for the trajectory repetition, F_{sf} is the force set-point for the control of the tool feed rate, F_{so} is the force set-point for the control of the tool orientation.

the control parameter of the human mimicking deburring algorithm are reported in Table 2.

4.1. *Results and Discussion*

A first important result is the reduction of the cycle time between T1 and T2 decreased from 157.4[s] to 76.9[s] (see Figure 11 and 12). Despite the multiple trajectories repetition of T2 experiment, the removal of thin layers of material allows to execute T2 with a feed rate 40 times higher than the one used in T1. Furthermore, the feed rate used during the execution of T2 is a conservative choice, while the feed rate used for T1 is the maximum feed rate that can be used to avoid spindle stall.

On the one hand, the force peaks registered during the execution of T2 (see Figure 12) are higher than the force peaks registered during the execution of T1 (see Figure 11). On the other hand, the reduction of the feed rate allows to quickly reduce the interaction forces, even to hold the robot and to detach the deburring tool from the workpiece. Hence, a new trajectory can be planned and executed with an offset along the y axis of tool frame $\{t\}$. Furthermore, looking at the force signal of Figure 12,

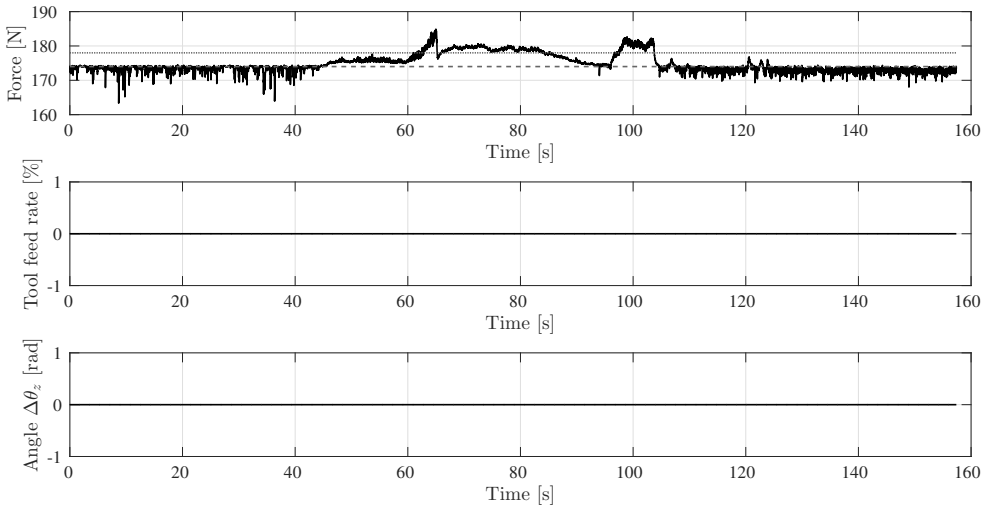

Figure 11. T1 experiment. The first panel reports the force measured along y direction of tool frame $\{t\}$ with a black continuous line, while the setpoints F_{sf} and F_{so} are displayed respectively with a dark grey dotted line and a light grey dotted line. The second panel reports the percentage of feed rate f_v while the third panel reports the tool angle θ_z deviation *w.r.t.* the nominal value.

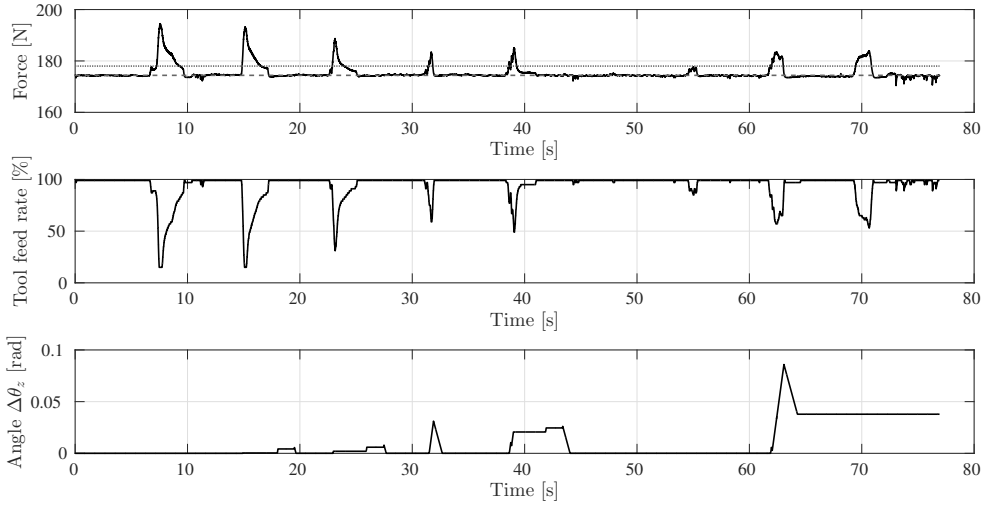

Figure 12. T2 experiment. The first panel reports the force measured along y direction of tool frame $\{t\}$ with a black continuous line, while the setpoints F_{sf} and F_{so} are displayed respectively with a dark grey dotted line and a light grey dotted line. The second panel reports the percentage of feed rate f_v while the third panel reports the tool angle θ_z deviation *w.r.t.* the nominal value.

repetition after repetition the force peaks gradually decrease up to disappear.

Additionally, the control of tool orientation θ_z and consequently the arm kinematics configuration, allow to reduce the robot stiffness when the force increase stabilizing the deburring process.

A qualitative analysis of the workpiece surface highlights also better performance of T2 *w.r.t.* T1. Indeed, as shown in Figure 13, the workpiece surface after the burr removal results not uniform with scratches and holes because of the tool vibrations due to the low feed rate. Furthermore, in the experiment T1, part of the surface is burned because of the high temperature reached from the long presence of the deburring tool on the workpiece surface. On the contrary, as shown in Figure 14, the workpiece

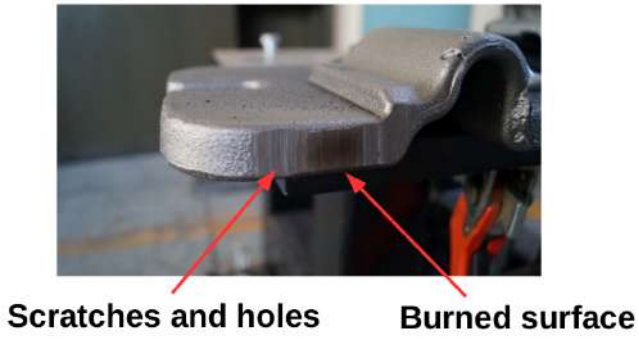

Figure 13. T1 experiment results: workpiece surface after burr removal using a constant feed rate approach.

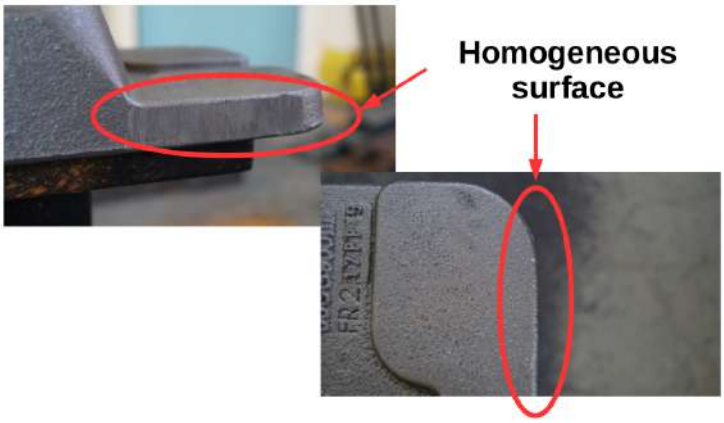

Figure 14. T2 experiment results: workpiece surface after burr removal exploiting the human mimicking control strategy.

surface obtained from T2 appears uniform without scratches or holes. Experiments demonstrates the effectiveness of the proposed control strategy achieving good results in terms of finishing surface quality and in terms of cycle time reduction.

The CDSA-AR1 was validated *a posteriori* on the experiment T2 to demonstarte the effectiveness of the algorithm. The measure of F_f acquired during the experiment was resampled at 100 [Hz]. The dimension of the window N was fixed to 25 samples, the threshold value of α (see Equation 3) to detect the changepoint was fixed to 1.001 in order to reduce the noise effect. The result obtained by the use of the CDSA-AR1 on the force signal F_f is reported in Figure 15. The changepoints are all detected, furthermore, from a rough analysis of the graph it is possible to compute the delay introduced from the CDSA-AR1. In fact, the average time for the changepoint detection is $\cong 0.16$ [s]. Such delay, with a feedrate of 40 [mm/s], determines a progress of the deburring tool of 6.4 [mm] before detecting the presence of a burr and before stopping the robot movement. It is worth noting that the delay introduced from the use of the absolute threshold F_{th} is $\cong 0.27$ [s].

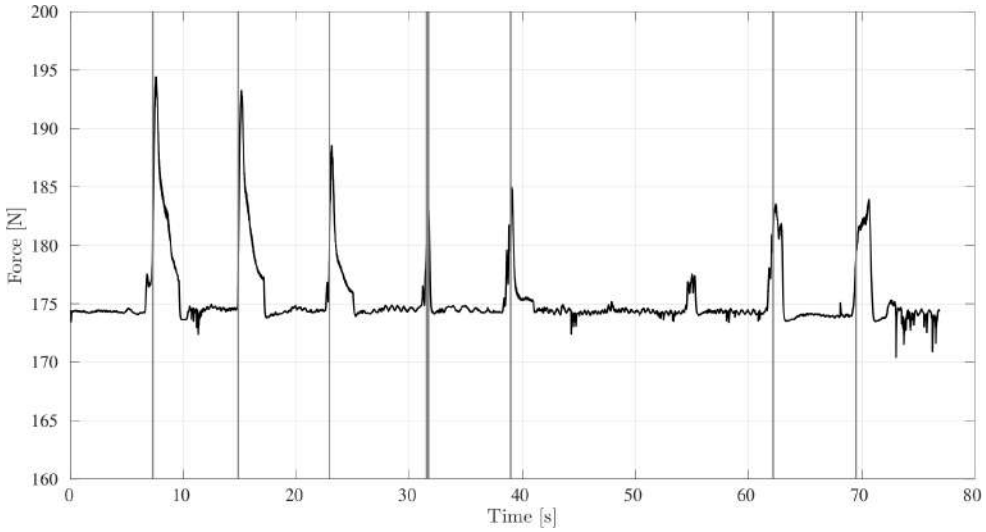

Figure 15. CDSA-AR1 applied on the force feedback signal recorded during the experiment T2.

5. Conclusions

In this paper, it was introduced a human mimicking control strategy applied on a deburring task. The proposed algorithm allows the robotic system to remove big burrs made by hard material by removing thin layer of material each time. Indeed, on the base of a force feedback, provided from a 1-axis load cell, the nominal deburring trajectory is adjusted and deformed making multiple repetition until the nominal deburring path is completed and the burr removed. The removal of thin layers of material allows the robot to operate at high feedrates avoiding spindle stall and without exciting elastic effects on the mechanical structure of the system. The effectiveness of the algorithm is demonstrated comparing the proposed method with a standard industrial approach. The results demonstrates a reduction of the cycle time equal to half of the time. Finally, the paper describes a method for the force changepoints detection based on the analysis of the stability of an AR1 model. This solution avoids the tuning of an absolute force threshold but allows the use of an adimensional threshold independent from the material and from the burr dimensions.

Concerning future works, a force/torque virtual sensor (Simoni et al. 2017) could be used to estimate the contact force, also along the other directions with respect to the measuring direction of the load cell. Moreover, the digital robot model can be integrated with a model of the technological process (Leonesio et al. 2012) to predict the process forces and the robot deflection, then use this information in the changepoints algorithm. Finally, the human-mimicking control algorithm could be generalized to address other material removal process, for example polishing, and to address different kinds of materials (both hard and soft materials).

6. Acknowledgements

The work is partially supported by Flexicast project EU-FP7-2012-NMP-ICT-FoF. Special thanks to J. C. Dalberto laboratory technician, of CNR-ITIA involved in setting up the experiments.

References

J. Pandremenos, C. Doukas, P. Stavropoulos, and G. Chryssolouris. Machining with robots: A critical review. In *Proceedings of the 7th International Conference on Digital Enterprise Technology (DET 2011)*, pages 614–621, Athens (GR), 2011.

C. Lehmann, M. Pellicciari, M. Drust, and J. W. Gunnink. *Machining with Industrial Robots: The COMET Project Approach*, pages 27–36. Springer Berlin Heidelberg, Berlin, Heidelberg, 2013. ISBN 978-3-642-39223-8. .

N.S. Rea Minango and C.J. Espindola Ferreira. Combining the STEP-NC standard and forward and inverse kinematics methods for generating manufacturing tool paths for serial and hybrid robots. *International Journal of Computer Integrated Manufacturing*, 30(11): 1203–1223, 2017. .

I. Iglesias, M.A. Sebastián, and J.E. Ares. Overview of the state of robotic machining: Current situation and future potential. *Procedia Engineering*, 132:911 – 917, 2015. ISSN 1877-7058. .

F.J. Xi, T. Chen, and S. Guo. Robotic Polishing and Deburring. In *Comprehensive Materials Finishing*, volume 1-3, pages 121–153. Elsevier, 2017. ISBN 9780128032503. .

G. Berselli, M. Gadaleta, A. Genovesi, M. Pellicciari, M. Peruzzini, and R. Razzoli. *Engineering methods and tools enabling reconfigurable and adaptive robotic deburring*, pages 655–664. Springer International Publishing, 2017. ISBN 978-3-319-45781-9. .

ATI. Robotic Deburring Tools. `http://www.ati-ia.com/Products/deburr/deburring_home.aspx`, 2016.

E. Villagrossi, C. Cenati, N. Pedrocchi, M. Beschi, and Lorenzo Molinari Tosatti. Flexible robot-based cast iron deburring cell for small batch production using single-point laser sensor. *The International Journal of Advanced Manufacturing Technology*, pages 1–14, 2017. ISSN 1433-3015. .

E. Abele, M. Weigold, and S. Rothenb??cher. Modeling and identification of an industrial robot for machining applications. *CIRP Annals - Manufacturing Technology*, 56(1):387–390, 2007. ISSN 00078506. .

E. Abele, J. Bauer, S. Rothenbücher, M. Stelzer, and O. Stryk. Prediction of the tool displacement by coupled models of the compliant industrial robot and the milling process. In *Proceedings of the International Conference on Process Machine Interaction*, pages 223–230, Sept 2008.

L. Cen and S.N. Melkote. Effect of Robot Dynamics on the Machining Forces in Robotic Milling. *Procedia Manufacturing*, 10:486–496, 2017. ISSN 23519789. .

H. Kazerooni. Automated robotic deburring using impedance control. *Control Systems Magazine, IEEE*, 8(1):21–25, Feb 1988. ISSN 0272-1708. .

B. M. Kramer and S. S. Shim. Development of a system for robotic deburring. *Robotics and Computer Integrated Manufacturing*, 7(3):291 – 295, 1990. ISSN 0736-5845. .

G. M. Bone, M. A. Elbestawi, R. R. Lingarkar, and L. L. Liu. Force control for robotic deburring. *ASME Journal of Dynamic Systems, Measurement, and Control*, 113(3):395–400, 1991. .

G. Duelen, H. Munch, D. Surdilovic, and J. Timm. Automated force control schemes for robotic deburring: Development and experimental evaluation. In *Proceedings of the International Conference on Industrial Electronics, Control, Instrumentation, and Automation, 1992. Power Electronics and Motion Control*, pages 912–917 vol.2, Nov 1992. .

T. Thomessen, O. J. Elle, J. L. Larsen, T. Andersen, J. E. Pedersen, and T. K. Lien. Automatic programming of grinding robot. *Modeling, Identification and Control*, 14(2):93–105, 1993. .

G. Ziliani, A. Visioli, and G. Legnani. A mechatronic approach for robotic deburring. *Mechatronics*, 17(8):431 – 441, 2007. ISSN 0957-4158. .

Wang X., Y. Wang, and Y. Xue. Adaptive control of robotic deburring process based on impedance control. In *Proceedings of the IEEE International Conference on Industrial Informatics*, pages 921–925, Aug 2006. .

ABB. Function Package for Force Control. `http://new.abb.com/`

products/robotics/application-equipment-and-accessories/flexfinishing/function-package-for-force-control, 2016.

Fanuc. Utilizing Force Sensors in Your Robotic Applications. http://robot.fanucamerica.com/robotics-articles/force-sensors-in-robot-applications.aspx, 2016.

M. Jonsson, A. Stolt, A. Robertsson, S. Gegerfelt, and K. Nilsson. On force control for assembly and deburring of castings. *Production Engineering*, 7(4):351–360, 2013. ISSN 1863-7353. .

H. Zhang, H. Chen, N. Xi, G. Zhang, and J. He. On-line path generation for robotic deburring of cast aluminum wheels. In *Intelligent Robots and Systems, 2006 IEEE/RSJ International Conference on*, pages 2400–2405, Oct 2006. .

H.C. Song, B.S. Kim, and J.B. Song. Tool path generation based on matching between teaching points and cad model for robotic deburring. In *Proceedings of the IEEE/ASME International Conference on Advanced Intelligent Mechatronics (AIM)*, pages 890–895, July 2012. .

H.C. Song and J.B. Song. Precision robotic deburring based on force control for arbitrarily shaped workpiece using cad model matching. *International Journal of Precision Engineering and Manufacturing*, 14(1):85–91, 2013. ISSN 2005-4602. .

M. M. Daniali and G. Vossoughi. Intelligent active vibration control of constrained manipulaors in robotic deburring. In *2009 International Conference on Industrial Mechatronics and Automation*, pages 76–80, May 2009. .

A. Kuss, M. Drust, and A. Verl. Detection of workpiece shape deviations for tool path adaptation in robotic deburring systems. *Procedia CIRP*, 57:545 – 550, 2016. ISSN 2212-8271. . Factories of the Future in the digital environment - Proceedings of the 49th CIRP Conference on Manufacturing Systems.

OSRF - Open Source Robotic Foundation. ROS - Robot Operating System. www.ros.org, 2016.

Open Source Project. ROS Industrial. www.rosindustrial.org, 2016.

M. Lavielle. Using penalized contrasts for the change-point problem. *Signal Processing*, 85(8): 1501 – 1510, 2005. ISSN 0165-1684. .

R. Killick, P. Fearnhead, and I. A. Eckley. Optimal detection of changepoints with a linear computational cost. In *Journal of the American Statistical Association*, pages 1590–1598, 2012. .

L. Simoni, E. Villagrossi, M. Beschi, A. Marini, N. Pedrocchi, L. Molinari Tosatti, G. Legnani, and A. Visioli. On the use of a temperature based friction model for a virtual force sensor in industrial robot manipulators. In *Proceedings of the IEEE International Conference on Emerging Technologies and Factory Automation*, Limassol (CY), 2017.

M. Leonesio, P. Parenti, A. Cassinari, G. Bianchi, and M. Monno. A Time-Domain Surface Grinding Model for Dynamic Simulation. *Procedia CIRP*, 4:166–171, 2012. ISSN 22128271. .